International Journal of Information, Control and Computer Sciences
ISSN: 2517-9942
Vol:8, No:7, 2014

Generalized Mean-field Theory of Phase Unwrapping via Multiple Interferograms

Yohei Saika

***Abstract*—**On the basis of Bayesian inference using the maximizer of the posterior marginal estimate, we carry out phase unwrapping using multiple interferograms via generalized mean-field theory. Numerical calculations for a typical wave-front in remote sensing using the synthetic aperture radar interferometry, phase diagram in hyper-parameter space clarifies that the present method succeeds in phase unwrapping perfectly under the constraint of surface- consistency condition, if the interferograms are not corrupted by any noises. Also, we find that prior is useful for extending a phase in which phase unwrapping under the constraint of the surface-consistency condition. These results are quantitatively confirmed by the Monte Carlo simulation.

***Keywords*—**Bayesian inference, generalized mean-field theory, phase unwrapping, statistical mechanics.

I. Introduction

FOR a long time, researchers have been studying Bayesian inference in the field of information science and technology. Especially, in the initial stage of the development of this field, Bayesian inference [1], [2] has been applied to the fundamental problems which are related to error-correcting codes and image restoration. Then, the Bayesian inference has been utilized for various problems in many research fields.

On the other hand, a lot of researchers have studied remote sensing using the synthetic aperture radar (SAR) interferometry [3], [4]. Main objective of this field is to acquire information on various objects and phenomena appearing on the surface of the earth. Then, researchers have constructed optical instruments using the interferometer. Also, the researchers have proposed a technique called as phase unwrapping to reconstruct original wave-fronts via the interferogram which was observed by the SAR interferometry. The important point of this problem is to remove residues in the observed interferogram. For this purpose, various techniques have been proposed for this problem, such as the least squares estimation [3], [4], the MAP estimation [5], simulated annealing [6] and Bayesian approach [7], [8] for this problem. In recent years, some researchers have investigated this problem form the statistical mechanical point of view. Saika and Nishimori [9] have proposed a method for phase retrieval based on the Bayesian inference using the maximizer of the posterior marginal (MPM) estimate. They found that the MPM estimate succeeded in phase retrieval with high degree of accuracy, if we used an appropriate model.

Recently, Saika and Uezu [10] have proposed a method for wave-front reconstruction in remote sensing using the SAR interferometry. They first carried out phase unwrapping from the observed interferogram due to the Bayesian inference via the MPM estimate using the statistical mechanics of the three-state Ising model, and then reduced noises from the wave-fronts reconstructed by the MPM estimate. They have found that the MPM estimate was effective for phase unwrapping under the constraint of surface-consistency condition at each plaquette, and that the accuracy was improved by introducing the process of noise reduction using an appropriate model.

In this paper, we construct a method of phase unwrapping using multiple interferograms based on the Bayesian inference using the MPM estimate which corresponds to the statistical mechanics of the three-state Ising model. Here, in order to construct a practical and useful technique for phase unwrapping, we apply a generalized version of the mean-field theory using the three-state Ising model to phase unwrapping using the multiple interferograms. In this study, we try this approach with a hope that the accuracy of phase unwrapping may be improved by probabilistic information processing utilizing fluctuations around the MAP solution, and that the accuracy is also improved with the use of multiple interferograms. Here, from the viewpoint of statistical mechanics, we then evaluate static property from a phase diagram in the hyper-parameter space. Here, we clarify that the present method is useful for phase unwrapping under the constraint of the surface- consistency condition. Also, we find that the prior information is useful for extending the PU phase in which the original wave-front is reconstructed perfectly/accurately. Next, we investigate dynamic property for phase unwrapping using the multiple interferograms. We find that the MPM estimate smoothly carries out phase unwrapping at the point located near the upper phase boundary of the PU phase. Then, these results obtained by the generalized mean-field theory is almost same as those obtained by the Monte Carlo simulation with respect to the artificial wave-front approximating the realistic one in remote sensing using the SAR interferometry.

The content of this paper is organized as follows. First, we show our formulation for phase unwrapping using the multiple interferograms on the basis of the Bayesian inference using the MPM estimate using the generalized mean-field theory. Then, we examine the static property of the present method from the PU phase of the phase diagram in the hyper-parameter space. Last part is devoted to summary and discussion.

II. Bayesian Inference

For a long time, a lot of researchers have been investigating

Yohei Saika is with the Gunma National College of Technology, 580 Toriba, Maebashi 371-8530, Japan (phone: +81-27-254-9256; fax: +81-27-254-9009; e-mail: saika@ice.gunma-ct.ac.jp).

information sciences related to problems of image restoration and error-correcting codes. Then, researchers have developed various techniques on the basis of the Bayesian inference in various fields, such as information communication and information reconstruction. In the following part of this chapter, we show the general formulation on the Bayesian inference using the maximizer of the posterior marginal (MPM) estimate.

First, we consider a set of original images $\{\xi_{i,j}\}$ ($\xi_{i,j}$=0, 1, i,j=1,…,L) generated by the assumed true prior which is expressed as the probability $\Pr(\{\xi_{i,j}\})$. Here, $\xi_{i,j}$=0,…,255 and i, j=1,…,L. In this study, we assume the Boltzmann distribution:

$$\Pr_{s}(\{\xi_{i,j}\}) = \frac{1}{Z_s}\exp\left[-\frac{J_s}{T_s}\sum_{\text{n.n.}}(\xi_{i,j}-\xi_{i',j'})^2\right] \quad (1)$$

for the true prior. Next, each image is rewritten into a corrupted image $\{\tau_{i,j}\}$ by some noises expressed as the conditional probability $\Pr(\{\tau_{i,j}\}|\{\xi_{i,j}\})$. Here, $\tau_{i,j}$=0, 1, as we assume the additive white Gaussian noise as

$$\Pr_{\text{cor}}(\{\tau_{i,j}\}|\{\xi_{i,j}\}) = \frac{1}{(2\pi\sigma_s^2)^{L^2/2}}\exp\left[-\frac{1}{(2\sigma_s^2)^{L^2/2}}\sum_{(i,j)}(\tau_{i,j}-\xi_{i,j})^2\right] \quad (2)$$

where σ_s^2 is the variance of the Gaussian noise. Then, with the use of information on each corrupted image $\{\tau_{i,j}\}$, we carry out image restoration based on the Bayesian inference using the MPM estimate. For this purpose, we consider a set of variables $\{z_{i,j}\}$ which are arranged on the square lattice, where $z_{i,j}$=0, 1, i,j=1,…,L. In this method, with the use of the set of variables $\{z_{i,j}\}$, we restore image so as to maximize the marginal posterior probability as

$$\hat{z}_{i,j} = \arg\max_{z_{i,j}=0,\ldots,255}\sum_{\{z\}\neq z_{i,j}}\Pr(\{\tau_{i,j}\}|\{z_{i,j}\}) \quad (3)$$

Here, the posterior probability is estimated based on the Bayes-formula using the likelihood and the model of the true prior. Here, we assume the likelihood as

$$\Pr_{\text{li}}(\{\tau_{i,j}\}|\{z_{i,j}\}) = \frac{1}{(2\pi\sigma^2)^{L^2/2}}\exp\left[-\frac{1}{(2\sigma^2)^{L^2/2}}\sum_{(i,j)}(\tau_{i,j}-\xi_{i,j})^2\right] \quad (4)$$

Then, we assume the model of the true prior as

$$\Pr_{\text{m}}(\{z_{i,j}\}) = \frac{1}{Z_s}\exp\left[-\frac{J}{T_m}\sum_{\text{n.n.}}(z_{i,j}-z_{i',j'})^2\right] \quad (5)$$

Here, σ, J and T_{m} are the parameters which should be determined appropriately.

Here, it has been known that the optimal performance is realized under the conditions:

$$\Pr_{\text{m}}(\{z_{i,j}\}) = \Pr_{\text{tr}}(\{z_{i,j}\}) \quad (6)$$

$$\Pr_{\text{li}}(\{\tau_{i,j}\}|\{z_{i,j}\}) = \Pr_{\text{cor}}(\{\tau_{i,j}\}|\{z_{i,j}\}) \quad (7)$$

These equations indicate that the optimal performance is realized, if information both on the true prior and the conditional property of corruption are clarified.

III. General Formulation

Here, as shown in Fig. 1, we show our formulation for phase unwrapping using multiple interferograms based on the Bayesian inference using the generalized mean-field theory. As shown in Fig. 2, we first consider an original wave-front $\{\xi_{i,j}\}$ which is arranged on the square lattice, where $0<\xi_{i,j}<\infty$ and i, j=1,…,L. The original wave-front $\{\xi_{i,j}\}$ is then corrupted by some noises, when the wave-front is carried through a noisy transmission to optical measurement systems. Here, as shown in Fig. 3, receivers observe a set of interferograms restricted to the principal interval from $-\pi$ to $+\pi$:

$$\eta_{i,j}(k) = \text{mod}(\xi_{i,j}+n_{i,j}(k)+\pi, 2\pi)-\pi \quad . \quad (8)$$

Here, $\{n_{i,j}(k)\}$ (k=1,…,N, i,j=1,…,L) are some noises onto the original wave-front. Then, we derive two set of principal phase differences both along the x- and y-axis:

$$\tau_{i,j}^{k,x} = \text{mod}(\eta_{i+1,j}^{k}-\eta_{i,j}^{k}+n_{i,j}^{x}(k)+\pi, 2\pi)-\pi \ , \quad (9)$$

$$\tau_{i,j}^{k,y} = \text{mod}(\eta_{i,j+1}^{k,y}-\eta_{i,j}^{k,y}+n_{i,j}^{y}(k)+\pi, 2\pi)-\pi \quad (10)$$

from the interferograms $\{\eta_{i,j}(k)\}$. Here, $n^{x}_{i,j}(k)$ and $n^{y}_{i,j}(k)$ are some noises onto the phase differences restricted to the principal interval. Here, we note that the residue pattern is shown in Fig. 4. As shown in Fig. 5 (a), aliasing does not occur, if the absolute value of the wave-front slope is less than π at each sampling point. On the other hand, as shown in Fig. 5 (b), aliasing occurs, if the absolute values of the wave-front slopes are more than π at several sampling points.

Next, we carry out phase unwrapping from these phase differences $\{\tau^{x}_{i,j}\}$ and $\{\tau^{y}_{i,j}\}$ based on the Bayesian inference using the MPM estimate corresponding to statistical mechanics of three-state Ising model $\{n^{x}_{i,j}\}$ and $\{n^{y}_{i,j}\}$ on the square lattice in Fig. 6. Here, $n^{x}_{i,j}$=-1, 0, +1, i = 1,…,L-1, j = 1,…,L and $n^{y}_{i,j}$ = -1, 0, +1, i =1,…,L, j = 1,…,L-1. This model is used to remove residues which appear in the set of the interferograms $\{\eta_{i,j}(k)\}$. In this method, we carry out phase unwrapping so as to maximize the marginal posterior probability as

$$\hat{n}^{x}_{i,j} = \arg\max_{n^{x}_{i,j}=-1,0,+1}\sum_{\{n^{x}\}\neq n^{x}_{i,j}}\sum_{\{n^{y}\}}\Pr(\{n^{x}\},\{n^{y}\}|\{\tau^{x}\},\{\tau^{y}\}) \ , \quad (11)$$

$$\hat{n}^{y}_{i,j} = \arg\max_{n^{y}_{i,j}=-1,0,+1}\sum_{\{n^{x}\}}\sum_{\{n^{y}\}\neq n^{y}_{i,j}}\Pr(\{n^{x}\},\{n^{y}\}|\{\tau^{x}\},\{\tau^{y}\}), \quad (12)$$

where the posterior probabilities in these equations can be estimated based on the Bayes formula:

$$\begin{aligned}&\Pr(\{n^{x}\},\{n^{y}\}|\{\tau^{x}\},\{\tau^{y}\})\\ &\quad\propto \Pr(\{n^{x}\},\{n^{y}\})\Pr(\{\tau^{x}\},\{\tau^{y}\}|\{n^{x}\},\{n^{y}\}).\end{aligned} \quad (13)$$

In this study, we assume the model prior so as to suppress the

occurrence of residues in the interferograms. The explicit form of the model prior is given as

$$\Pr(\{n^x\},\{n^y\}) = \frac{1}{Z_m}\exp\left[-\frac{h}{T_m}\sum_{(i,j)}\left\{|n^x_{i,j}|^p + |n^y_{i,j}|^p\right\}\right], \quad (14)$$

where the h, T_m and p are hyper-parameters which we should tune appropriately. Then, we assume the likelihood so as to enhance smooth structures, as seen from patterns of wave-fronts which are typical in remote sensing using the SAR interferometry. The explicit form of the likelihood used here is

$$\Pr(\{\tau^x\},\{\tau^y\}\,|\,\{n^x\},\{n^y\}) \propto \exp\left[-\frac{1}{T_m}\left\{J\cdot H_{sm}(\{n^x\},\{n^y\}) + \Gamma\cdot H_{scc}(\{n^x\},\{n^y\})\right\}\right], \quad (15)$$

where

$$H_{sm}(\{n^x\},\{n^y\}) = \sum_{k=1}^{N}\sum_{(i,j)}\left\{\tau^x_{i+1,j}-\tau^x_{i,j}+2\pi(n^x_{i+1,j}-n^x_{i,j})\right\}^2 + \sum_{k=1}^{N}\sum_{(i,j)}\left\{\tau^y_{i,j+1}-\tau^y_{i,j}+2\pi(n^y_{i,j+1}-n^y_{i,j})\right\}^2 + \alpha\sum_{k=1}^{N}\sum_{(i,j)}\left\{\tau^x_{i,j+1}-\tau^x_{i,j}+2\pi(n^x_{i,j+1}-n^x_{i,j})\right\}^2 + \alpha\sum_{k=1}^{N}\sum_{(i,j)}\left\{\tau^x_{i+1,j}-\tau^x_{i,j}+2\pi(n^x_{i+1,j}-n^x_{i,j})\right\}^2 \quad (16)$$

and

$$H_{scc}(\{\tau^x\},\{\tau^y\}\,|\,\{n^x\},\{n^y\}) = \sum_{k=1}^{N}\sum_{(i,j)}\left\{\tau^x_{i,j}+\tau^y_{i+1,j}-\tau^x_{i,j+1}-\tau^y_{i,j}+2\pi(n^x_{i,j}+n^y_{i+1,j}-n^x_{i,j+1}-n^y_{i,j})\right\}^2. \quad (17)$$

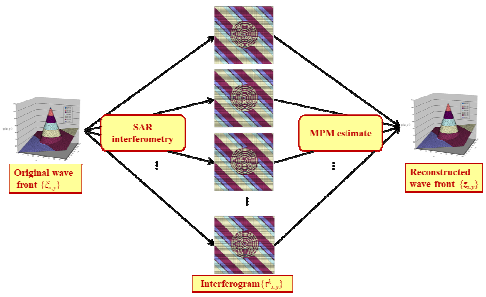

Fig. 1 General formulation for phase unwrapping using multiple interferograms

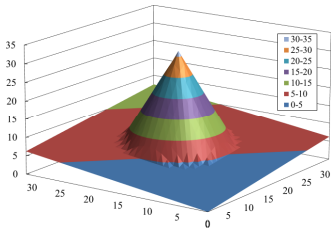

Fig. 2 An original information which approximates the wave-front in remote sensing using the SAR interferometry

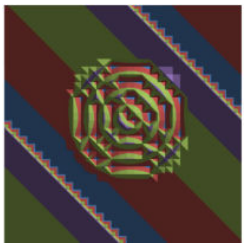

Fig. 3 An interferogram of the original wave-front in Fig. 2

Fig. 4 A residue pattern of the interferogram in Fig. 3.

In this study, in order to estimate posterior probability, we utilize the generalized version of the mean-field theory which is established in the field of statistical mechanics. Here, we utilize the effective version of the mean-field Hamiltonian, such as

$$H^x_{eff}(\{n^x\},\{n^y\};\{m^x\},\{m^y\}) = H^x_1(\{n^x\},\{n^y\}) + H^x_{2x}(\{n^x\},\{n^y\}) + H^x_{2y}(\{n^x\},\{n^y\}) + H^x_3(\{n^x\},\{n^y\}), \quad (18)$$

where

$$\begin{aligned} &H^x_1(\{n^x\},\{n^y\}) \\ &= J\sum_{k=1}^{Ns}(\tau^{k,x}_{i,j}-\tau^{k,x}_{i+1,j}+2\pi(n^x_{i,j}-n^x_{i+1,j}))^2 \\ &+ J\sum_{k=1}^{Ns}(\tau^{k,x}_{i,j}-\tau^{k,x}_{i-1,j}+2\pi(n^x_{i,j}-n^x_{i-1,j}))^2 \\ &+ J\sum_{k=1}^{Ns}(\tau^{k,y}_{i,j-1}-\tau^{k,y}_{i,j}+2\pi(n^y_{i,j-1}-n^y_{i,j}))^2 \\ &+ J\sum_{k=1}^{Ns}(\tau^{k,y}_{i+1,j-1}-\tau^{k,y}_{i+1,j}+2\pi(n^y_{i+1,j-1}-n^y_{i+1,j}))^2 \\ &+ \alpha J\sum_{k=1}^{Ns}(\tau^{k,x}_{i,j}-\tau^{k,x}_{i,j+1}+2\pi(n^x_{i,j}-n^x_{i,j+1}))^2 \\ &+ \alpha J\sum_{k=1}^{Ns}(\tau^{k,x}_{i,j}-\tau^{k,x}_{i,j-1}+2\pi(n^x_{i,j}-n^x_{i,j-1}))^2 \\ &+ \alpha J\sum_{k=1}^{Ns}(\tau^{k,y}_{i,j}-\tau^{k,y}_{i,j+1}+2\pi(n^y_{i,j}-n^y_{i,j+1}))^2 \\ &+ \alpha J\sum_{k=1}^{Ns}(\tau^{k,x}_{i,j}-\tau^{k,x}_{i,j-1}+2\pi(n^x_{i,j}-n^x_{i,j-1}))^2, \end{aligned} \quad (19)$$

$$
\begin{aligned}
&H^{x}_{2x}(\{n^{x}\},\{n^{y}\};\{m^{x}\},\{m^{y}\})\\
&=J\sum_{k=1}^{Ns}(\tau^{k,x}_{i+1,j}-\tau^{k,x}_{i+2,j}+2\pi(n^{x}_{i+1,j}-m^{x}_{i+2,j}))^{2}\\
&+J\sum_{k=1}^{Ns}(\tau^{k,x}_{i-1,j}-\tau^{k,x}_{i-2,j}+2\pi(n^{x}_{i-1,j}-m^{x}_{i-2,j}))^{2}\\
&+J\sum_{k=1}^{Ns}(\tau^{k,x}_{i,j+1}-\tau^{k,x}_{i+1,j+1}+2\pi(n^{x}_{i,j+1}-m^{x}_{i+1,j+1}))^{2}\\
&+J\sum_{k=1}^{Ns}(\tau^{k,x}_{i,j+1}-\tau^{k,x}_{i-1,j+1}+2\pi(n^{x}_{i,j+1}-m^{x}_{i-1,j+1}))^{2}\\
&+J\sum_{k=1}^{Ns}(\tau^{k,x}_{i,j-1}-\tau^{k,x}_{i+1,j-1}+2\pi(n^{x}_{i,j-1}-m^{x}_{i+1,j-1}))^{2}\\
&+J\sum_{k=1}^{Ns}(\tau^{k,x}_{i,j-1}-\tau^{k,x}_{i-1,j-1}+2\pi(n^{x}_{i,j-1}-m^{x}_{i-1,j-1}))^{2}\\
&+\alpha J\sum_{k=1}^{Ns}(\tau^{k,x}_{i,j+1}-\tau^{k,x}_{i,j+2}+2\pi(n^{x}_{i,j+1}-m^{x}_{i,j+2}))^{2}\\
&+\alpha J\sum_{k=1}^{Ns}(\tau^{k,x}_{i,j-1}-\tau^{k,x}_{i,j-2}+2\pi(n^{x}_{i,j-1}-m^{x}_{i,j-2}))^{2}\\
&+\alpha J\sum_{k=1}^{Ns}(\tau^{k,x}_{i+1,j}-\tau^{k,x}_{i+1,j+1}+2\pi(n^{x}_{i+1,j}-m^{x}_{i+1,j+1}))^{2}\\
&+\alpha J\sum_{k=1}^{Ns}(\tau^{k,x}_{i+1,j}-\tau^{k,x}_{i+1,j-1}+2\pi(n^{x}_{i+1,j}-m^{x}_{i+1,j-1}))^{2}\\
&+\alpha J\sum_{k=1}^{Ns}(\tau^{k,x}_{i-1,j}-\tau^{k,x}_{i-1,j+1}+2\pi(n^{x}_{i-1,j}-m^{x}_{i-1,j+1}))^{2}\\
&+\alpha J\sum_{k=1}^{Ns}(\tau^{k,x}_{i-1,j}-\tau^{k,x}_{i-1,j-1}+2\pi(n^{x}_{i-1,j}-m^{x}_{i-1,j-1}))^{2}\\
&+\alpha J\sum_{k=1}^{Ns}(\tau^{k,x}_{i,j+2}-\tau^{k,x}_{i+1,j+2}+2\pi(m^{x}_{i,j+2}-m^{x}_{i+1,j+2}))^{2}\\
&+\alpha J\sum_{k=1}^{Ns}(\tau^{k,x}_{i,j-2}-\tau^{k,x}_{i+1,j-2}+2\pi(m^{x}_{i,j-2}-m^{x}_{i+1,j-2}))^{2}.
\end{aligned}
\tag{20}
$$

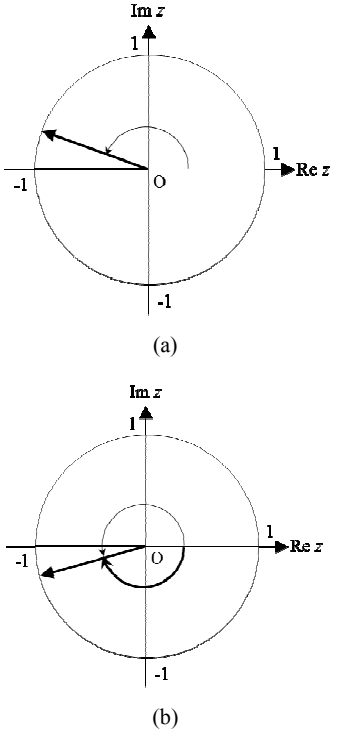

Fig. 5 Shannon's sampling theorem, (a) aliasing does not occur at every sampling point, if each absolute value of the wave-front slope is less than π (b) aliasing occurs, if several absolute values of the wave-fronts are more than π

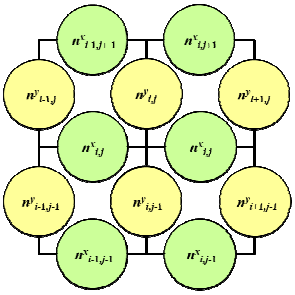

Fig. 6 Square lattice used for this problem

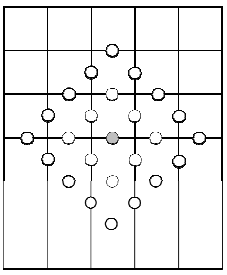

Fig. 7 Lattice for one of the effective Hamiltonian $H^{x}(\{n^{x}\}, \{n^{y}\} \mid \{m^{x}\}, \{m^{y}\})$ used for the generalized mean-field theory. Here, ● is the target lattice point. Then, ○ is the lattice point where the Q-Ising spin $\{n^{x}\}/\{n^{y}\}$ is arranged. Next, ○ is the lattice point where the effective field $\{m^{x}\}/\{m^{y}\}$ is arranged

$$
\begin{aligned}
&H^{x}_{2y}(\{n^{x}\},\{n^{y}\})\\
&=J\sum_{k=1}^{Ns}(\tau^{k,y}_{i,j}-\tau^{k,y}_{i,j+1}+2\pi(n^{y}_{i,j}-m^{y}_{i,j+1}))^{2}\\
&+J\sum_{k=1}^{Ns}(\tau^{k,y}_{i,j-1}-\tau^{k,y}_{i,j-2}+2\pi(n^{y}_{i,j-1}-m^{y}_{i,j-2}))^{2}\\
&+J\sum_{k=1}^{Ns}(\tau^{k,y}_{i+1,j}-\tau^{k,y}_{i+1,j+1}+2\pi(n^{y}_{i+1,j}-m^{y}_{i+1,j+1}))^{2}\\
&+J\sum_{k=1}^{Ns}(\tau^{k,y}_{i+1,j-1}-\tau^{k,y}_{i-1,j-2}+2\pi(n^{y}_{i+1,j-1}-m^{y}_{i+1,j-2}))^{2}\\
&+J\sum_{k=1}^{Ns}(\tau^{k,y}_{i+2,j}-\tau^{k,y}_{i+2,j-1}+2\pi(m^{y}_{i+2,j}-m^{y}_{i+2,j-1}))^{2}\\
&+J\sum_{k=1}^{Ns}(\tau^{k,y}_{i-1,j}-\tau^{k,y}_{i-1,j+1}+2\pi(m^{y}_{i-1,j}-m^{y}_{i-1,j+1}))^{2}\\
&+J\sum_{k=1}^{Ns}(\tau^{k,y}_{i+2,j}-\tau^{k,y}_{i+2,j-1}+2\pi(m^{y}_{i+2,j}-m^{y}_{i+2,j-1}))^{2}\\
&+J\sum_{k=1}^{Ns}(\tau^{k,y}_{i-1,j}-\tau^{k,y}_{i-1,j-1}+2\pi(m^{y}_{i-1,j}-m^{y}_{i-1,j-1}))^{2}\\
&+\alpha J\sum_{k=1}^{Ns}(\tau^{k,y}_{i,j}-\tau^{k,y}_{i-1,j}+2\pi(n^{y}_{i,j}-m^{y}_{i-1,j}))^{2}\\
&+\alpha J\sum_{k=1}^{Ns}(\tau^{k,y}_{i,j-1}-\tau^{k,y}_{i-1,j-1}+2\pi(n^{y}_{i,j-1}-m^{y}_{i-1,j-1}))^{2}\\
&+\alpha J\sum_{k=1}^{Ns}(\tau^{k,y}_{i+1,j}-\tau^{k,y}_{i+2,j}+2\pi(n^{y}_{i+1,j}-m^{y}_{i+2,j}))^{2}\\
&+\alpha J\sum_{k=1}^{Ns}(\tau^{k,y}_{i+1,j-1}-\tau^{k,y}_{i+2,j-1}+2\pi(n^{y}_{i+1,j-1}-m^{y}_{i+2,j-1}))^{2}\\
&+\alpha J\sum_{k=1}^{Ns}(\tau^{k,y}_{i,j+1}-\tau^{k,y}_{i,j+2}+2\pi(m^{y}_{i,j+1}-m^{y}_{i,j+2}))^{2}\\
&+\alpha J\sum_{k=1}^{Ns}(\tau^{k,y}_{i,j-1}-\tau^{k,y}_{i,j-2}+2\pi(m^{y}_{i,j-1}-m^{y}_{i,j-2}))^{2}
\end{aligned}
\tag{21}
$$

and

$$
\begin{aligned}
&H_3^x(\{m^x\},\{m^y\}) \\
&= \Gamma\sum_{k=1}^{Ns}(\tau_{i,j}^{k,x}+\tau_{i+1,j}^{k,y}-\tau_{i,j+1}^{k,x}-\tau_{i,j}^{k,y}+2\pi(n_{i,j}^x+n_{i+1,j}^y-n_{i,j+1}^x-n_{i,j}^y))^2 \\
&+\Gamma\sum_{k=1}^{Ns}(\tau_{i,j-1}^{k,x}+\tau_{i+1,j-1}^{k,y}-\tau_{i,j}^{k,x}-\tau_{i,j-1}^{k,y}+2\pi(n_{i,j-1}^x+n_{i+1,j-1}^y-n_{i,j}^x-n_{i,j-1}^y))^2 \\
&+\Gamma\sum_{k=1}^{Ns}(\tau_{i+1,j}^{k,x}+\tau_{i+2,j}^{k,y}-\tau_{i+1,j+1}^{k,x}-\tau_{i+1,j}^{k,y}+2\pi(n_{i+1,j}^x+m_{i+2,j}^y-m_{i+1,j+1}^x-n_{i+1,j}^y))^2 \\
&+\Gamma\sum_{k=1}^{Ns}(\tau_{i+1,j-1}^{k,x}+\tau_{i+2,j-1}^{k,y}-\tau_{i+1,j}^{k,x}-\tau_{i+1,j-1}^{k,y}+2\pi(m_{i+1,j-1}^x+m_{i+2,j-1}^y-n_{i+1,j}^x-n_{i+1,j-1}^y))^2 \\
&+\Gamma\sum_{k=1}^{Ns}(\tau_{i-1,j}^{k,x}+\tau_{i,j}^{k,y}-\tau_{i-1,j+1}^{k,x}-\tau_{i-1,j}^{k,y}+2\pi(n_{i-1,j}^x+n_{i,j}^y-m_{i-1,j+1}^x-m_{i-1,j}^y))^2 \\
&+\Gamma\sum_{k=1}^{Ns}(\tau_{i-1,j-1}^{k,x}+\tau_{i,j-1}^{k,y}-\tau_{i-1,j}^{k,x}-\tau_{i-1,j-1}^{k,y}+2\pi(m_{i-1,j-1}^x+n_{i,j-1}^y-n_{i-1,j}^x-m_{i-1,j-1}^y))^2 \\
&+\Gamma\sum_{k=1}^{Ns}(\tau_{i,j+1}^{k,x}+\tau_{i+1,j+1}^{k,y}-\tau_{i,j+2}^{k,x}-\tau_{i,j+1}^{k,y}+2\pi(n_{i,j+1}^x+m_{i+1,j+1}^y-m_{i,j+2}^x-m_{i,j+1}^y))^2 \\
&+\Gamma\sum_{k=1}^{Ns}(\tau_{i,j-2}^{k,x}+\tau_{i+1,j-2}^{k,y}-\tau_{i,j-1}^{k,x}-\tau_{i,j-2}^{k,y}+2\pi(m_{i,j-2}^x+m_{i+1,j-2}^y-n_{i,j-1}^x-m_{i,j-2}^y))^2.
\end{aligned}
\tag{22}
$$

Here, as seen from Fig. 7, $\{m^x_{i,j}\}$ and $\{m^y_{i,j}\}$ are the set of the effective fields which are defined on the boundary of the effective Hamiltonian. Next, the effective Hamiltonian $H^y_{\text{eff}}(\{n^x\},\{n^y\};\{m^x\},\{m^y\})$ is then constructed in the similar way to the above case. In this method, these variables should be determined by following self- consistency conditions as

$$
m_{i,j}^x=\frac{\sum_{\{n^x\}}\sum_{\{n^y\}}\exp\left[-\beta_m H_{MF}^x(\{n^x\},\{n^y\};\{m^x\},\{m^y\})\right]n_{i,j}^x}{\sum_{\{n^x\}}\sum_{\{n^y\}}\exp\left[-\beta_m H_{MF}^x(\{n^x\},\{n^y\};\{m^x\},\{m^y\})\right]}, \tag{23}
$$

$$
m_{i,j}^y=\frac{\sum_{\{n^x\}}\sum_{\{n^y\}}\exp\left[-\beta_m H_{MF}^y(\{n^x\},\{n^y\};\{m^x\},\{m^y\})\right]n_{i,j}^y}{\sum_{\{n^x\}}\sum_{\{n^y\}}\exp\left[-\beta_m H_{MF}^y(\{n^x\},\{n^y\};\{m^x\},\{m^y\})\right]}. \tag{24}
$$

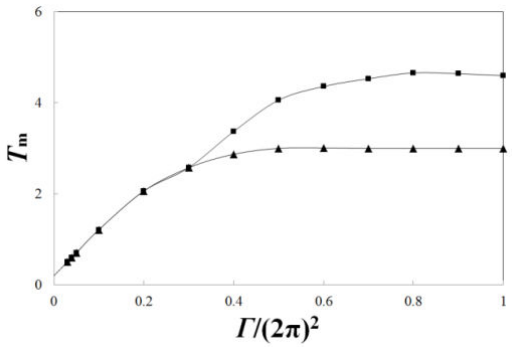

Fig. 8 Mean square error as a function of parameter T_m due to the MPM estimate via 8 interferograms which are not corrupted by any noises. Here, ▲ denotes the upper phase boundary of the PU phase, if σ=0, J=1, α=0 and h=0. Then, ■ denotes the upper phase boundary of the PU phase, if σ=0, J=1, α=0 and h=1

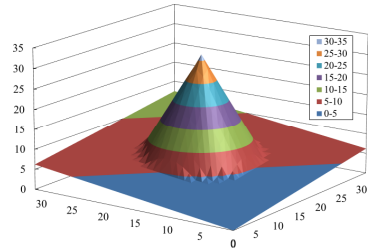

Fig. 9 A wave-front perfectly reconstructed from the interferogram in Fig. 3 by the generalized mean- field theory

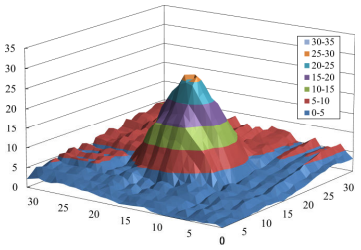

Fig. 10 A wave-front reconstructed from the interferograms in Fig. 3 by the generalized mean-field theory using the single interferogram

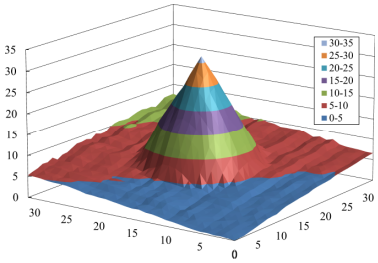

Fig. 11 A wave-front reconstructed by the mean-field theory using 8 interferograms

Here, β_m (=1/T_m) is a hyper-parameter which expresses the inverse temperature. Here, s study, we used the above model prior and likelihood following the previous papers [10],[11]. Then, the reconstructed wave-front $\{z_{i,j}\}$ is obtained as

$$
z_{i,j}=z_{0,0}+\sum_{l=1}^{i-1}(\tau_{l,0}^x+2\pi\hat{n}_{l,0}^x)+\sum_{m=1}^{j-1}(\tau_{i,m}^y+2\pi\hat{n}_{i,m}^y). \tag{25}
$$

If we clarify the performance of the present method, we evaluate the accuracy of the present method based on the performance measure using the mean square error:

$$
\sigma=\frac{1}{L^2}\sum_{i=1}^{L}\sum_{j=1}^{L}(z_{i,j}-\xi_{i,j})^2 \tag{26}
$$

This becomes zero, if the wave-front is reconstructed perfectly.

IV. Performance

In this chapter, we show the performance estimation on the MPM estimate for phase unwrapping from the statistical mechanical point of view. Here, we show the performance of

the generalized mean-field theory from the phase diagram in the hyper-parameter space. Then, we clarify the efficiency of our model for the problem of phase unwrapping with respect to the single wave-front in Fig. 2.

In this simulation, we utilize an original wave-front $\{\xi_{i,j}\}$ in Fig. 2 which is a typical example in remote sensing via the SAR interferometry. Then, the original wave-front $\{\xi_{i,j}\}$ is corrupted by the Gaussian noise $\{n_{i,j}(0, \sigma^2)\}$. Here, σ^2 is the variance of the Gaussian noise, if the wave-front is carried through the noisy channel, such as atmosphere. Next, we observe multiple interferograms $\{\zeta_{i,j}(k)\}$ from the corrupted wave-front $\{\eta_{i,j}\}$. Then, we derive two sets of phase differences $\{\tau^{k,x}_{i,j}\}$ and $\{\tau^{k,y}_{i,j}\}$ in the principal interval from the corrupted wave-front $\{\eta^{k}_{i,j}\}$. Then, on the basis of the Bayesian inference using the mean-field theory, we carry out phase unwrapping via multiple interferograms $\{\eta^{k}_{i,j}\}$ (Fig. 3) by making use of the generalized mean-field theory due to the three-state Ising model on the square lattice. In order to clarify the efficiency of the present method, we evaluate the performance measure using the mean square error.

In this estimation, in order to clarify the static property of the present method, we describe the phase diagram which shows the stability of the PU phase in the hyper-parameter spaces, where the PU phase is a phase in which the present method succeeds in phase unwrapping perfectly, if the observed interferograms are not corrupted by any noises. As shown in Figs. 8 and 9, we find that the present method succeeds in phase unwrapping perfectly under the constraint of the surface-consistency condition, and that the prior information is available of extending the PU phase under the constraint of the surface consistency condition. Also, we find that the structure of the phase diagram in Fig. 7 is almost same as that obtained by the Monte Carlo simulation [11] for the wave-front which is typical in remote sensing using the SAR interferometry. Then, as shown in Figs. 10 and 11, we find that the accuracy in phase unwrapping is improved with the increase in the number of the interferograms observed by the SAR interferometry, even if the interferograms are corrupted by some noises. These results mean that the generalized mean-field theory proposed in this paper realizes almost same performance as the Bayesian inference using the MPM estimate due to the Monte Carlo simulation for the wave-front in remote sensing using the SAR interferometry.

V. Summary and Discussion

In previous chapters, after we have overviewed the statistical mechanical Bayesian inference in information science and technology, such as image restoration and error-correcting codes, we have outlined the methodologies of the statistical mechanical Bayesian inference for these problems. In this paper, we have shown the Bayesian inference through the typical example of image restoration with respect to grayscale images. Here, we have shown that thermal fluctuations around the ground state (the MAP solution) are useful for the Bayesian inference with high degree of accuracy. In the following part, we have shown our original research on the generalized mean-field theory for the problem of phase unwrapping via multiple interferograms. Here, we have first constructed the technique of phase unwrapping via multiple interferograms based on the generalized mean-field theory. Then, we have examined static property of the present method for this problem. We have clarified the static property of the present method from the phase diagram in the hyper-parameter space. We have clarified that the Bayesian inference using the MPM estimate succeeded in phase unwrapping perfectly under the constraint of the surface-consistency condition, and that the prior information is useful for extending the PU phase under the constraint of the surface-consistency condition. Next, we have clarified that the accuracy of the generalized mean-field theory was improved with the increase in the number of the interfeorgrams use for phase unwrapping.

As a future problem, we are going to apply the present method on the basis of the generalized mean-field theory via the three-state Ising model to realistic problem in remote sensing using the SAR interferometry.

References

[1] C. M. Bishop, *Pattern Recognition and Machine Learning*. New York: Springer, 2007.
[2] J. Albert, *Bayesian Computation with R, Second edit.*, New York, Dordrecht, etc.: Springer, 2009.
[3] D. C. Ghiglia and M. D. Pritt, *Two-Dimensional Phase Unwrapping The ory Algorithms and Software*, New York: Wiley, 1998.
[4] R. M. Goldstein and H. A. Zebker, "Interferometric radar mapping of oce an currents," *Nature*, Vol. 328, pp. 707-709, 1987.
[5] J. L. Marroquin and M. Rivera, Quadratic regularization functions for phase unwrapping, Journal of Optical Society of America, Vol.
[6] L. Guerriero, G. Nico, G. Pasquariello, and A. Stramaglia, A new regulari zation scheme for phase unwrapping, Applied Optics, Vol. 37, No. 14, 19 98, pp. 3053-3058.
[7] G. Nico, G. Plubinskas and M. Datcu, Bayesian approach to phase unwra pping: Theoretical Study, IEEE Transactions. Signal Processing, Vol. 48 (4), 2000, pp. 2524-2556.
[8] H. Nishimori, *Theory of spin glasses and information;An introduction,* O xford, London, 2001.
[9] K. Tanaka, "Statistical mechanical approach to image processing," *Journ al of Physics A: Mathematical and General*, Vol. 35(37), pp.R31-R150, 2 002.
[10] Y. Saika and H. Nishimori, "Statistical mechanical approach to phase retr ieval using the Q-Ising model", *Progress Theoretical Physics Supplement*, Vol.157, pp. 292-295, 2005.
[11] Y. Saika and T. Uezu, "Statistical Mechanical Approach to Phase Unwrap ping in Remote Sensing Using the Synthetic Aperture Radar Interferomet ry", *Interdisciplinary Information Sciences*, Vol. 19(1), pp. 73-78, 2013.